

Mixed Convection in a Composite System Bounded by Vertical Walls

N. Srivastava¹ and A. K. Singh²

Department of Mathematics, Banaras Hindu University, Varanasi-221005, India

Email: ¹neetusri_81@rediffmail.com, ²ashok@bhu.ac.in

(Received March 30, 2009; accepted September 6, 2009)

ABSTRACT

A combined convection process between two parallel vertical infinite walls, containing an incompressible viscous fluid layer and a fluid saturated porous layer has been presented analytically. There is a vertical axial variation of temperature in the upward direction along the walls. The Brinkman extended Darcy model is applied to describe the momentum transfer in the porous region. The viscosity of the fluid layer and the effective viscosity of the porous layer are assumed to be different. Also the thermal conductivities of both fluid and porous layers are assumed to be different. The graphs and tables have been used to distinguish the influence of distinct parameters on the velocity and skin-friction. It is determined that the velocity is intensified on making greater the temperature difference between the walls while increment in the viscosity ratio (porous/fluid) parameter diminishes the velocity of the fluid. It has been observed that the numerical values of the skin-frictions have an increasing tendency with the increment in the values of temperature difference between the walls while decreasing tendency with the increment in the viscosity ratio parameter (porous/fluid).

Keywords: Mixed convection, composite system, effective viscosity, porous media, Brinkman model

NOMENCLATURE

A	temperature gradient along the wall	u'	velocity along the x' -direction
Da	Darcy number	u	velocity along x -direction in non-dimensional form
d'	distance of interface	x'	vertical coordinate
d	distance of interface in non-dimensional form	x	vertical coordinate in non-dimensional form
g	acceleration due to gravity	y'	horizontal coordinate
H	distance between the vertical walls	y	horizontal coordinate in non-dimensional form
k'	permeability of the porous medium	Greek symbols	
P'	pressure	α	thermal diffusivity
Q	constant including pressure gradient term	β	coefficient of thermal expansion
Ra	Rayleigh number	μ_f	dynamic viscosity of the fluid
Rc	ratio of thermal conductivities	μ_{eff}	effective viscosity of the porous region
Rv	ratio of effective viscosity to the dynamic viscosity	θ	temperature in non-dimensional form
T'_0	reference temperature	ρ	density
T'_1	temperature at the wall $y'=0$	Subscripts	
		f	fluid layer
		p	porous layer

1. INTRODUCTION

The phenomena of mixed or combined convection arise when both free and forced convection simultaneously occur. Free convection means the motion which arises due to buoyancy effects while forced convection results due to any external force. An analytical solution of mixed convective flow between vertical parallel walls for higher Rayleigh number has been presented by Beckett and Friend (1984). A study of mixed convection flows between parallel plate channels has been presented by Aung and Worku (1986). An exact analytical solution of mixed convective flow on a permeable vertical cylinder in a saturated porous medium has been given by Ramanaiah and Malarvizhi (1990). Singh *et al.* (1993) have presented numerically the three dimensional free convection in a cavity as a result of side heating. An analytical study of natural convective flow in a composite system containing fluid and porous layers between two vertical walls has been presented by Paul *et al.* (1998). Paul *et al.* (1999) have further extended in case of unsteady natural convective flow.

The problem of mixed convection in a porous medium bounded by two vertical walls has been done by Mishra *et al.* (2002). Nobari and Beshkani (2007) have studied numerically the mixed convective flow in a vertical channel by applying finite difference method based on projection algorithm. The mixed convective flow between vertical parallel plates has been solved numerically by Guillet *et al.* (2007). A numerical study of mixed convective flow in rotating ducts has been done by Chiu *et al.* (2007). Ahmad *et al.* (2008) has investigated numerically the mixed convection along vertical thin needles. An analytical solution as well as a numerical solution is obtained by Barletta (2008) for the mixed convective flow in an inclined tube. The problem of unsteady turbulent flow and mixed convection has been presented numerically by Perng and Wu (2008). A numerical solution of mixed convective flow across a confined square cylinder has been acquired by Dhiman *et al.* (2008). A numerical result of the problem of mixed convective flow along a vertical slender cylinder has been given by Singh and Roy (2008) and the corresponding result for unsteady mixed convective flow has been shown by Singh *et al.* (2008). The problem of mixed convection of a nano fluid containing water and Al_2O_3 in horizontal and inclined tubes with constant heat flux has been examined numerically by Akbari *et al.* (2008).

Zanchini (2008) has given an analytical solution of mixed convective flows in a vertical annulus having constant wall temperatures. For the mixed convective flow of a viscoelastic fluid over a horizontal circular cylinder a numerical result has been presented by Anwar *et al.* (2008). Using Keller-box method, a numerical study of mixed convective flow in a porous medium has been done by Ishak *et al.* (2008). The problem of mixed convective flow from a wavy surface has been investigated experimentally by Kuhn and Rohr (2008). The study of turbulent mixed convection from vertical, parallel plate channels is discussed by Balaji *et al.* (2008) by applying asymptotic considerations. The effect of surface mass transfer on mixed convective

flows is exhibited by giving numerical solution by Datta *et al.* (2008). Mohammed (2008) has given an experimental result of mixed convective flow in a vertical circular tube under constant heat flux boundary conditions. The problem of mixed convection in a rectangular enclosure is numerically solved by Saha *et al.* (2008) using finite element method. Sharma and Singh (2009) have shown the effects of variable thermal conductivity and heat source/sink on flow of a viscous incompressible electrically conducting fluid past a semi-infinite flat plate by using shooting method. A numerical solution is carried out by Mahanti and Gaur (2009) in order to show the effect of varying viscosity and thermal conductivity on steady natural convective flow of a viscous incompressible fluid by applying the Runge-Kutta fourth order method with shooting technique.

The study of mixed convection in a composite system has its importance in various fields such as aeronautical engineering, petroleum reservoir engineering, the technologies of paper, geothermal energy, storage system etc. The motive of contemplating this study is to present an analytical solution of mixed convection between two vertical walls containing a fluid and a porous material when the temperature of the walls varies vertically upward. Brinkman extended Darcy model is used to model the flow in porous region. For fully developed laminar flow, the velocity has only one component in vertical direction. The viscosity of the fluid layer and the effective viscosity of the porous layer are taken to be different. Three different analytical solutions of the model have been obtained depending on the values of Darcy number, viscosity ratio parameter, thermal conductivity ratio parameter and Rayleigh number. Finally effects of various physical parameters have been shown by using graphs and tables.

2. MATHEMATICAL FORMULATION

In the given problem a steady fully developed laminar free convective flow between two infinite vertical walls filled with a fluid layer and a fluid saturated porous layer is considered as shown in Fig. 1. The interface of fluid and porous layers is taken permeable so that fluid can flow from one layer to other. The x' -axis is taken in the vertical direction while y' -axis is taken in the horizontal direction. The walls at $y' = 0$ and $y' = H$ are maintained at the temperatures $T_0 + Ax'$ and $T_1 + Ax'$ respectively, where x' is the distance measured vertically in the upward direction. Under usual Boussinesq's approximation, the governing equations in the reference of the considered problem in non-dimensional form are derived as follows:

For fluid region (Beckett and Friend (1984)):

$$\frac{d^2 u_f}{dy^2} + Ra\theta_f = -1, \quad (1)$$

$$\frac{d^2 \theta_f}{dy^2} - u_f = 0, \quad (2)$$

For porous region (Mishra *et al.* (2002)):

$$Ru \frac{d^2 u_p}{dy^2} + Ra\theta_p - \frac{1}{Da} u_p = -1, \quad (3)$$

$$Rc \frac{d^2 \theta_p}{dy^2} - u_p = 0. \tag{4}$$

The corresponding boundary and matching conditions in non-dimensional form are acquired as follows (Singh *et al.* (1993)):

$$\begin{aligned} \text{at } y = 0, \quad & u_f = 0, \quad \theta_f = 0, \\ \text{at } y = 1, \quad & u_p = 0, \quad \theta_p = \frac{T_1' - T_0'}{AHQ} = Q, \\ \text{at } y = d, \quad & u_f = u_p, \quad \frac{du_f}{dy} = Rv \frac{du_p}{dy}, \\ \text{at } y = d, \quad & \theta_f = \theta_p, \quad \frac{d\theta_f}{dy} Rc = \frac{d\theta_p}{dy}. \end{aligned} \tag{5}$$

The non-dimensional quantities used in the above equations are obtained as follows:

$$\begin{aligned} y &= \frac{y'}{d}, & u_f &= \frac{u'_f H}{Q \alpha_f}, & u_p &= \frac{u'_p H}{Q \alpha_f}, \\ \theta_f &= \frac{\theta'_f}{AHQ}, & \theta_p &= \frac{\theta'_p}{AHQ}, & Rv &= \frac{\mu_{eff}}{\mu_f}, \\ Da &= \frac{K'}{H^2}, & Rc &= \frac{\alpha_p}{\alpha_f}, & Ra &= \frac{\rho g \beta H^4}{\alpha_f \mu_f}, \\ Q &= \frac{\rho H^3}{\alpha_f \mu_f} \left\{ \left(-\frac{1}{\rho} \frac{dP'}{dx'} + g \right) + g \beta A x' \right\}. \end{aligned} \tag{6}$$

Eliminating θ_f from Eqs. (1) and (2), we get a fourth order differential equation in u_f as

$$\frac{d^4 u_f}{dy^4} + Rau_f = 0 \tag{7}$$

while eliminating θ_p from Eqs. (3) and (4) a fourth order differential equation in u_p is obtained as

$$\frac{d^4 u_p}{dy^4} - \frac{1}{Da} \frac{d^2 u_p}{dy^2} + \frac{Ra}{Rc} u_p = 0, \tag{8}$$

whose auxiliary roots are obtained as given below:

$$\begin{aligned} m_1, m_2 &= \pm \sqrt{\frac{1+S}{2DaRv}}, \\ m_3, m_4 &= \pm \sqrt{\frac{1-S}{2DaRv}}, \end{aligned} \tag{9}$$

where

$$S = \sqrt{1 - \frac{4RaRvDa^2}{Rc}}.$$

It is obvious from the auxiliary roots described in Eq. (9), that the solution for the velocity and temperature fields depends on the values of Ra , Rv , Da and Rc and there arises three different cases which are as follows:

Case1. When $1 - \frac{4RaRvDa^2}{Rc} > 0$;

In this case S will be a real number. Solving Eqs. (7) and (8) with their proper boundary conditions the

solution for u_f , θ_f , u_p and θ_p are obtained as given below:

$$\begin{aligned} u_f &= e^{Ny} (C_1 \cos Ny + C_2 \sin Ny) \\ &+ e^{-Ny} (C_3 \cos Ny + C_4 \sin Ny), \end{aligned} \tag{10}$$

$$\begin{aligned} \theta_f &= -\frac{1}{Ra} - \frac{2N^2}{Ra} [e^{Ny} (C_2 \cos Ny - C_1 \sin Ny) \\ &+ e^{-Ny} (C_3 \sin Ny - C_4 \cos Ny)], \end{aligned} \tag{11}$$

$$\begin{aligned} u_p &= (C_5 \cosh h_1 y + C_6 \sinh h_1 y) \\ &+ (C_7 \cosh h_2 y + C_8 \sinh h_2 y), \end{aligned} \tag{12}$$

$$\begin{aligned} \theta_p &= -\frac{1}{Ra} - \frac{Rv}{Ra} [C_5 h_1^2 \cosh h_1 y + C_6 h_1^2 \sinh h_1 y \\ &+ C_7 h_2^2 \cosh h_2 y + C_8 h_2^2 \sinh h_2 y] + \frac{1}{DaRa} \\ &[C_5 \cosh(h_1 y) + C_6 \sinh(h_1 y) + C_7 \cosh(h_2 y) \\ &+ C_8 \sinh(h_2 y)]. \end{aligned} \tag{13}$$

The above solutions are valid only for $0 < S < 1$.

Case2. When $1 - \frac{4RaRvDa^2}{Rc} = 0$;

In this case, the velocity and temperature fields in the fluid and porous region with the suitable boundary conditions are derived as

$$\begin{aligned} u_f &= e^{Ny} (C_1 \cos Ny + C_2 \sin Ny) \\ &+ e^{-Ny} (C_3 \cos Ny + C_4 \sin Ny), \end{aligned} \tag{14}$$

$$\begin{aligned} \theta_f &= -\frac{1}{Ra} - \frac{2N^2}{Ra} [e^{Ny} (C_2 \cos Ny - C_1 \sin Ny) \\ &+ e^{-Ny} (C_3 \sin Ny - C_4 \cos Ny)], \end{aligned} \tag{15}$$

$$\begin{aligned} u_p &= (C_5 + C_6 y) \cosh my \\ &+ (C_7 + C_8 y) \sinh my, \end{aligned} \tag{16}$$

$$\begin{aligned} \theta_p &= -\frac{1}{Ra} - \frac{Rv}{Ra} [\{m^2 (C_1 + C_2 y) + 2mC_4\} \\ &\cosh my + \{m^2 (C_3 + C_4 y) + 2mC_2\} \sinh my] \\ &+ \frac{1}{DaRa} [(C_1 + C_2 y) \cosh my + (C_3 + C_4 y) \\ &\sinh my]. \end{aligned} \tag{17}$$

Case3. When $1 - \frac{4RaRvDa^2}{Rc} < 0$;

S will be imaginary in this case. The expressions for the velocity and temperature fields in the fluid and porous region with the corresponding boundary conditions are

$$\begin{aligned} u_f &= e^{Ny} (C_1 \cos Ny + C_2 \sin Ny) \\ &+ e^{-Ny} (C_3 \cos Ny + C_4 \sin Ny), \end{aligned} \tag{18}$$

$$\begin{aligned} \theta_f &= -\frac{1}{Ra} - \frac{2N^2}{Ra} [e^{Ny} (C_2 \cos Ny - C_1 \sin Ny) \\ &+ e^{-Ny} (C_3 \sin Ny - C_4 \cos Ny)], \end{aligned} \tag{19}$$

$$u_p = e^{\alpha y} (C_5 \cos \beta y + C_6 \sin \beta y) + e^{-\alpha y} (C_7 \cos \beta y + C_8 \sin \beta y), \quad (20)$$

$$\theta_p = -\frac{1}{Ra} + \frac{1}{DaRa} [e^{\alpha y} \beta \{C_5 \cos \beta y + C_6 \sin \beta y\} + e^{-\alpha y} \{C_7 \cos \beta y + C_8 \sin \beta y\}] - \frac{Rv}{Ra} [C_5 e^{\alpha y} \{(\alpha^2 - \beta^2) \cos \beta y - 2\alpha\beta \sin \beta y\} + C_6 e^{\alpha y} \{(\alpha^2 - \beta^2) \sin \beta y + 2\alpha\beta \cos \beta y\} + C_7 e^{-\alpha y} \{(\alpha^2 - \beta^2) \cos \beta y + 2\alpha\beta \sin \beta y\} + C_8 e^{-\alpha y} \{(\alpha^2 - \beta^2) \sin \beta y - 2\alpha\beta \cos \beta y\}]. \quad (21)$$

By using the Eqs. (10), (12), (14), (16), (18) and (20), expressions for the skin frictions in all three cases are derived as follows:

Case 1: When $1 - \frac{4RaRvDa^2}{Rc} > 0$;

$$\tau_1 = \left(\frac{du_f}{dy}\right)_{y=0} = N(C_1 + C_2 + C_4 - C_3), \quad (22)$$

$$\tau_2 = -\left(\frac{du_p}{dy}\right)_{y=1} = -(C_5 h_1 \sinh h_1 + C_6 h_1 \cosh h_1) + (C_7 h_2 \sinh h_2 + C_8 h_2 \cosh h_2). \quad (23)$$

Case 2: When $1 - \frac{4RaRvDa^2}{Rc} = 0$;

$$\tau_1 = -\left(\frac{du_f}{dy}\right)_{y=0} = -N(C_1 + C_2 + C_4 - C_3), \quad (24)$$

$$\tau_2 = \left(\frac{du_p}{dy}\right)_{y=1} = \{(C_5 + C_6)m + C_8\} \sinh m + \{(C_7 + C_8)m + C_6\} \cosh m. \quad (25)$$

Case 3: When $1 - \frac{4RaRvDa^2}{Rc} < 0$;

$$\tau_1 = \left(\frac{du_f}{dy}\right)_{y=0} = N(C_1 + C_2 + C_4 - C_3), \quad (26)$$

$$\tau_2 = -\left(\frac{du_p}{dy}\right)_{y=1} = e^\alpha \{C_5(\alpha \cos \beta - \beta \sin \beta) + C_6(\alpha \sin \beta + \beta \cos \beta) - e^\alpha C_8 \beta \cos \beta - \alpha \sin \beta - C_7 \beta \sin \beta + \alpha \cos \beta\} \quad (27)$$

The parameters used in the above equations are mentioned in the appendix.

3. RESULTS AND DISCUSSION

The influence of different physical parameters on the velocity field is depicted in the Figs. 2-3 for the case $S > 0$ while in the Figs. 4-6 for $S = 0$ and finally for

the case $S < 0$ in the Figs. 7-11. In Fig. 2 the effect of thermal conductivity ratio parameter Rc and viscosity ratio parameter Rv on the velocity field is shown. From the figure it can be clearly observed that the velocity is showing decreasing behavior with the increment in the values of Rv for all the values of Darcy number and this is expected due to impact of more viscous force. For $Da = 10^{-2}$, we can see that the effect of viscosity ratio parameter is negligible in the porous region. There is a decrement in the velocity on increasing the values of Rc in the fluid region while there is an increment in the velocity on increasing the values of Rc in the porous region. This phenomenon may occur due to more diffusion of heat in porous layer than fluid layer. In Fig. 3, the impact of pressure gradient constant Q , on the velocity field is hold to view. By examining the figure it has been noticed that the velocity becomes greater when the values of Q grow i.e., when the temperature difference between two walls is increasing. This is attributed to fact that velocity increases due to increment in the buoyancy force. In Fig. 4, the effect on the velocity field for the different values of Rc , Rv and Ra has been displayed when $S = 0$. The figure manifestly notifies that on increasing the value of Rv , the velocity decreases for all the values of Darcy number.

In Fig. 5, the relation between the fluid layer width d and the velocity has been presented to view. The figure completely notifies that with the increment in the fluid layer width d the velocity has growing nature for all the values of Darcy number. But for $Da = .05$, in the porous region there is a negligible influence of increment in fluid layer width. In Fig. 6, the variation in the velocity due to variation in the values of Q has been shown. It is clear from the figure that when $Q = 0$, that is when the temperature difference between two walls is zero then the flow is in the upward direction while for $Q > 0$, the flow is in the reverse direction.

In Fig. 7, the velocity profiles are shown for different values of Rc and Rv . It is remarkable from the figure that the effect of Rv on the velocity is to decrease it for all considered values of Darcy number. In this case also the velocity has a decreasing tendency in the fluid region while it is showing an increasing nature in the porous region on increasing the values of Rc . Also velocity is more apparent for $Da = 10^{-1}$ than that of $Da = 10^{-2}$. In Fig. 8, the effect of Rayleigh number Ra on the velocity field has been exhibited. It is quite remarkable from the figure that there is a decrement in the velocity due to increment in the values of Ra . In Fig. 8, the relation of velocity with the fluid layer width has been hold to view. From the figure it can be easily seen that the velocity varies in an increasing manner on increasing the fluid layer width. Figures 10 and 11 are given to describe the effect of Q on the velocity when Q hold the values close to zero and when Q hold the values greater than zero respectively. From both the Figs. 9 and 10, it is obvious that the velocity has increasing tendency with the increment in the values of Q for the all values of Darcy number.

At last, the numerical values of the skin-friction are computed on both the walls. Here, τ_1 and τ_2 represent

the numerical values of skin-friction on the walls $y = 0$ and $y = 1$ respectively and they are given in Tables 1, 2 and 3 for the different three cases $S > 0$, $S = 0$, and $S < 0$ respectively. From the Table 1, it is observed that on increasing the values of Rv and Ra both τ_1 and τ_2 are decreasing while increasing due to increment in the values of Darcy number, fluid layer width d and pressure gradient constant Q . The increment in the values of Rc makes decrement in τ_1 while it makes increment in τ_2 for all the values of Darcy number. From Table 2, it can be clearly viewed that the values of both τ_1 and τ_2 increase with the fluid layer width d and pressure gradient constant Q . From Table 3, it can be notified that both τ_1 and τ_2 have increasing tendency when the Darcy number Da , fluid layer width d and pressure gradient constant Q , tend to increment. With the increment in the values of Rc , τ_1 decreases while τ_2 increases. In this case, both τ_1 and τ_2 are showing decreasing behavior on increasing the values of Rv and Ra .

4. CONCLUSION

An analytical solution of mixed convection in a composite system containing a fluid layer and a porous layer bounded by vertical walls has been attained. It is resolved from the discussion that the velocity in both fluid and porous regions has decreasing tendency with the viscosity ratio parameter for all the cases which is due to fact that velocity decreases due to more viscous forces. The effect of the thermal conductivity ratio parameter is to enhance the velocity in the porous region while to diminish the velocity in the fluid region for all the values of Darcy number. Lastly, it has been concluded that numerical values of the skin friction exhibit an increasing behavior with the increment in the values of temperature difference between the walls, Darcy number and fluid layer width while the numerical values of skin friction are decreasing due to the viscosity ratio parameter and Rayleigh number.

REFERENCES

- Ahmad, S., N.M. Arifin, R. Nazar and I. Pop (2008). Mixed convection boundary layer flow along vertical thin needleless: Assisting and opposing flows. *International Communications in Heat and Mass Transfer* 35, 157-162.
- Akbari, M., A. Behzadmehr and F. Shahraki (2008). Fully developed mixed convection in horizontal and inclined tubes with uniform heat flux using nanofluid. *International Journal of Heat and Fluid Flow* 29, 545-556.
- Anwar, I., A. Norsarahaida and I. Pop (2008). Mixed convection boundary layer flow of a viscoelastic fluid over a horizontal circular cylinder. *International journal of Non-Linear Mechanics* 43, 814-821.
- Aung, W. and G. Worku (1986). Theory of fully developed, combined convection including flow reversal. *Journal of Heat Transfer* 108, 485-488.
- Balaji, C., M. Holling and H. Herwig (2008). A temperature wall functions for turbulent mixed convection from vertical, parallel plate channels. *International Journal of Thermal Sciences* 47, 723-729.
- Barletta, A. (2008). Parallel and non-parallel laminar mixed convection flow in an inclined tube: The effect of the boundary conditions. *International Journal of Heat and Fluid Flow* 29, 83-93.
- Beckett, P.M. and I.E. Friend (1984). Combined natural and forced convection between parallel walls: Developing flow at higher Rayleigh numbers. *International Journal of Heat and Mass Transfer* 27, 611-621.
- Chiu, H., J. Jang and W. Yan (2007). Combined mixed convection and radiation heat transfer in rectangular ducts rotating about a parallel axis. *International Journal of Heat and Mass Transfer* 50, 4229-4242.
- Datta, P., S.V. Subhashini and R. Ravindran (2009). Influence of surface mass transfer on mixed convection flows over non-isothermal horizontal flat plates. *Applied Mathematical Modelling* 33, 1285-1294.
- Dhiman, A.K., R.P. Chhabra and V. Eswaran (2008). Steady mixed convection across a confined square cylinder. *International Communications in Heat and Mass Transfer* 35, 47-55.
- Guillet, C., T. Mare and C.T. Nguye (2007). Application of a non-linear local analysis method for the problem of mixed convection instability. *International Journal of Non-Linear Mechanics* 42, 981-988.
- Ishak, A., R. Nazar and I. Pop (2008). Dual solutions in mixed convection flow near a stagnation point on a vertical surface in a porous medium. *International Journal of Heat and Mass Transfer* 51, 1150-1155.
- Kuhn, S. and P.R.V. Rohr (2008). Experimental investigation of mixed convective flow over a wavy wall. *International Journal of Heat and Fluid Flow* 29, 94-106.
- Mahanti, N.C. and P. Gaur (2009). Effects of varying viscosity and thermal conductivity on steady Free convective flow and heat transfer along an isothermal vertical plate in the presence of heat sink. *Journal of Applied Fluid Mechanics* 2, 23-28.
- Mishra, A.K., T. Paul and A.K. Singh (2002). Mixed convection in a porous medium bounded by two vertical walls. *Forschung im Ingenieurwesen* 67, 198-205.
- Mohammed, H.A. (2008). Laminar mixed convection heat transfer in a vertical circular tube under

buoyancy-assisted and opposed flow. *Energy Conservation and Management* 49, 2006-2015.

Nobari, M.R.H. (2007). A numerical study of mixed convection in a vertical channel flow impinging on a horizontal surface. *International Journal of Thermal Sciences* 46, 989-997.

Paul, T., A.K. Singh and G.R. Thorpe (1999). Transient natural convection in a vertical channel partially filled with a porous medium. *Journal of Mathematical Engineering in Industry* 7, 441-455.

Paul, T., B.K. Jha and A.K. Singh (1998). Free convection between vertical walls partially filled with porous medium. *Heat and Mass Transfer* 33, 515-519.

Perng, S. and H. Wu (2008). Numerical investigation of mixed convective heat transfer for unsteady turbulent flow over heated blocks in a horizontal channel. *International Journal of Thermal Sciences* 47, 620-632.

Ramanaiah, G. and G. Malarvizhi (1990). Unified treatment of free and mixed convection on a permeable vertical cylinder in a saturated porous medium. *Indian Journal of Technology* 28, 604-608.

Saha, S., M.A.H. Mamun, M.Z. Hossain and A.K.M.S. Islam (2008). Mixed convection in an enclosure with different inlet and exit configurations. *Journal of Applied Fluid Mechanics* 1, 78-93.

Sharma, P.R. and G. Singh (2009). Effects of variable thermal conductivity and heat source/ sink on MHD flow near a stagnation point on a linearly stretching sheet. *Journal of Applied Fluid Mechanics* 2, 13-21.

Singh, A.K., E. Leonardi and G.R. Thorpe (1993). 3-Dimensional natural convection in a confined fluid overlying a porous layer. *ASME Journal of Heat Transfer* 115, 631-638.

Singh, P.J. and S. Roy (2008). Mixed convection along a rotating vertical slender cylinder in an axial flow. *International Journal of Heat and Mass Transfer* 51, 717-723.

Singh, P.J., S. Roy and I. Pop (2008). Unsteady mixed convection from a rotating vertical slender cylinder in an axial flow. *International Journal of Heat and Mass Transfer* 51, 1423-1430.

Zanchini, E. (2008). Mixed convection with variable viscosity in a vertical annulus with uniform wall temperatures. *International Journal of Heat and Mass Transfer* 51, 30-40.

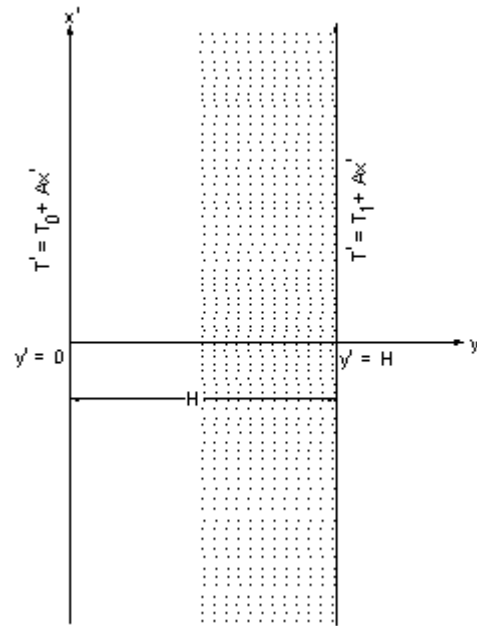


Fig. 1. Physical configuration of the model

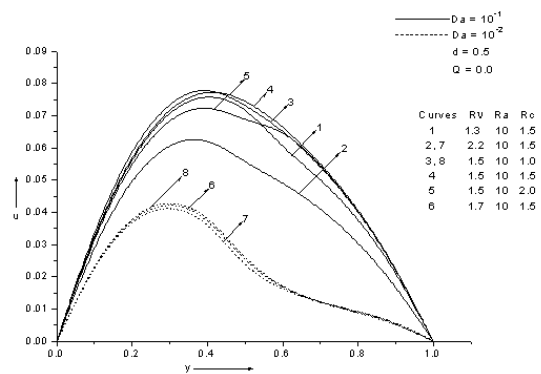


Fig. 2. Velocity profiles for different values of Rc and Rv (Case 1)

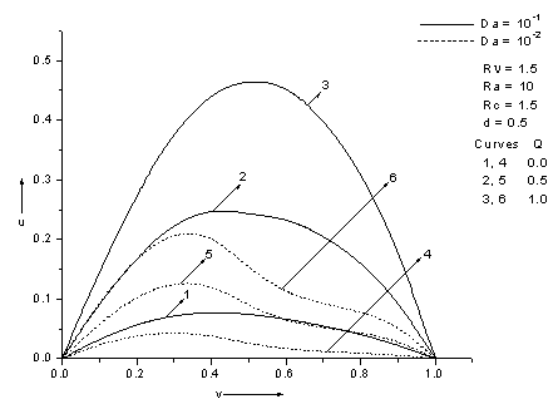


Fig. 3. Velocity profiles for different values Q (Case 1)

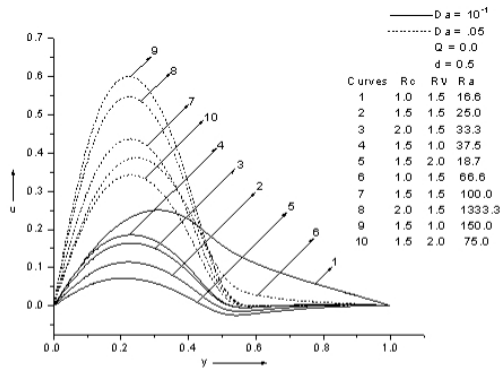


Fig. 4. Velocity profiles for different values of R_c , R_v and R_a (Case 2)

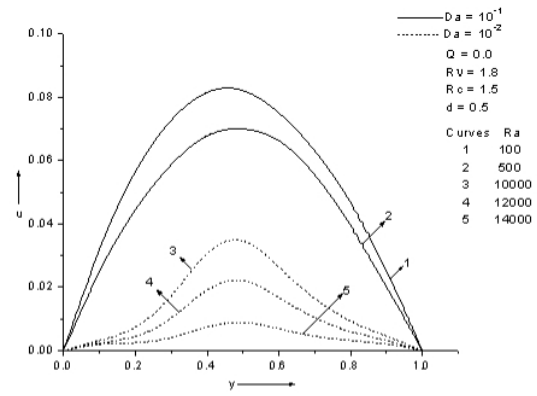


Fig. 8. Velocity profiles for different values of R_a (Case 3)

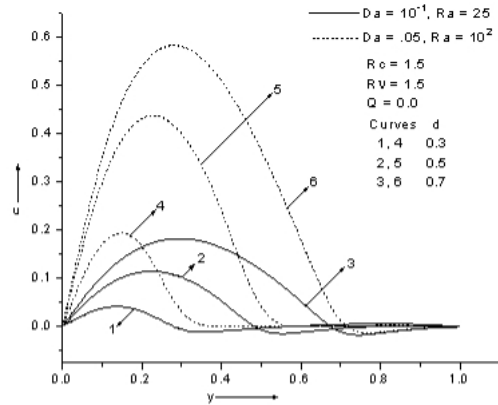


Fig. 5. Velocity profiles for different values of d (Case 2)

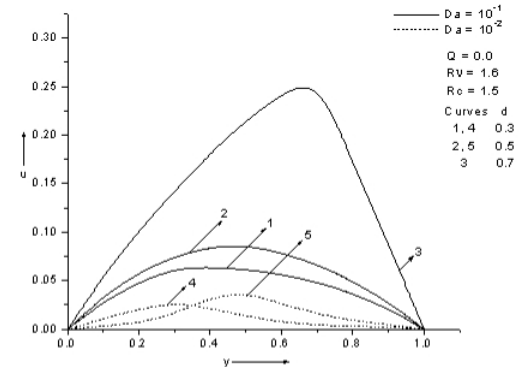


Fig. 9. Velocity profiles for different values of d (Case 3)

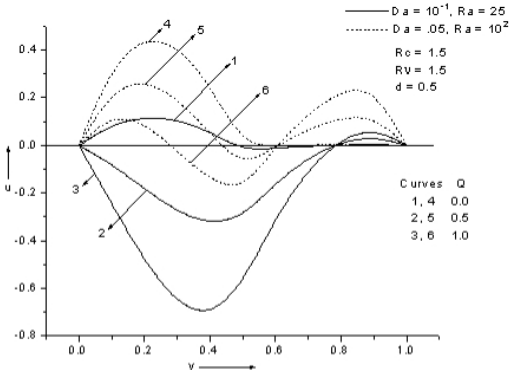


Fig. 6. Velocity profiles for different values of Q (Case 2)

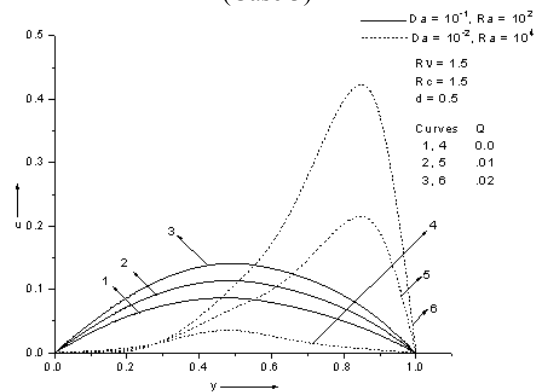


Fig. 10. Velocity profiles for different values of Q (Case 3)

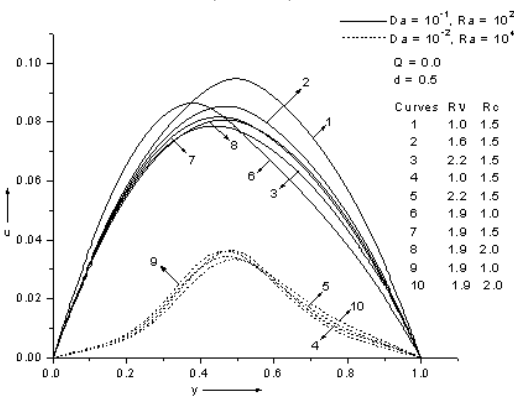


Fig. 7. Velocity profiles for different values of R_c and R_v (Case 3)

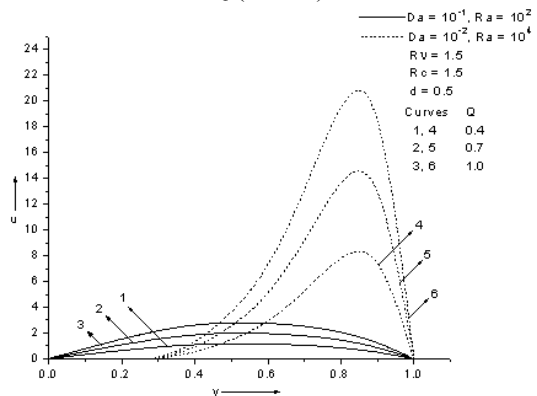


Fig. 11. Velocity profiles for different values of Q (Case 3)

Numerical values of skin frictions

Table1 Case 1

<i>Da</i>	Q	<i>Ra</i>	<i>Rv</i>	<i>Rc</i>	<i>d</i>	τ_1	τ_2
10 ⁻¹	0.0	10	1.3	1.5	0.5	0.386669	0.254900
	0.0	10	1.8	1.5	0.5	0.386578	0.220868
	0.0	10	1.5	1.0	0.5	0.401966	0.260029
	0.0	10	1.5	2.0	0.5	0.380595	0.260339
	0.0	15	1.5	1.5	0.5	0.366278	0.236119
	0.0	22	1.5	1.5	0.5	0.362220	0.225121
	0.0	10	1.5	1.5	0.3	0.348182	0.215806
	0.0	10	1.5	1.5	0.7	0.422484	0.280347
	0.5	10	1.5	1.5	0.5	0.998385	1.153310
10 ⁻²	1.0	10	1.5	1.5	0.5	1.540800	2.201330
	0.0	10	1.3	1.5	0.5	0.298580	0.091616
	0.0	10	1.8	1.5	0.5	0.293953	0.079290
	0.0	10	1.5	1.0	0.5	0.296468	0.085167
	0.0	10	1.5	2.0	0.5	0.296415	0.086007
	0.0	15	1.5	1.5	0.5	0.294816	0.085056
	0.0	22	1.5	1.5	0.5	0.290567	0.084347
	0.0	10	1.5	1.5	0.3	0.206724	0.081821
	0.0	10	1.5	1.5	0.7	0.393193	0.116738
	0.5	10	1.5	1.5	0.5	0.665799	0.464376
	1.0	10	1.5	1.5	0.5	1.034200	0.838864

Table2 Case 2

<i>Da</i>	Q	<i>Ra</i>	<i>Rv</i>	<i>Rc</i>	<i>d</i>	τ_1	τ_2
10 ⁻¹	0.0	25	1.5	1.5	0.3	0.206240	0.870637
	0.0	25	1.5	1.5	0.5	0.392751	1.056768
	0.0	25	1.5	1.5	0.7	0.964422	1.627459
	0.5	25	1.5	1.5	0.5	0.512209	1.323730
	1.0	25	1.5	1.5	0.5	0.631668	1.590671
	0.0	16.6	1.5	1.0	0.5	0.166228	0.950956
	0.0	33.3	1.5	2.0	0.5	2.100763	2.803604
	0.0	18.7	2.0	1.5	0.5	2.292225	1.237157
	0.0	20.8	1.5	1.8	0.5	0.886599	1.533033
.05	0.0	100	1.5	1.5	0.3	0.560225	0.532392
	0.0	100	1.5	1.5	0.5	0.727771	0.551913
	0.0	100	1.5	1.5	0.7	0.974949	0.578088
	0.5	100	1.5	1.5	0.5	0.929358	0.687462
	1.0	100	1.5	1.5	0.5	1.130945	0.823012
	0.0	133.3	1.5	2.0	0.5	0.537431	0.488496
	0.0	20.8	1.5	1.8	0.5	0.563640	0.497770

Table3 Case 3

<i>Da</i>	Q	<i>Ra</i>	<i>Rv</i>	<i>Rc</i>	<i>d</i>	τ_1	τ_2
10 ⁻¹	0.0	100	1.0	1.5	0.5	0.383112	0.386109
	0.0	100	2.0	1.5	0.5	0.379016	0.283202
	0.0	100	1.5	1.0	0.5	0.471167	0.236866
	0.0	100	1.5	2.0	0.5	0.372853	0.335647
	0.0	500	1.5	1.5	0.5	0.309017	0.226889
	0.0	900	1.5	1.5	0.5	0.291173	0.198156
	0.0	100	1.5	1.5	0.3	0.326804	0.249637
	0.0	100	1.5	1.5	0.7	0.587187	0.941567
	0.5	100	1.5	1.5	0.5	4.314726	8.213052
10 ⁻²	1.0	100	1.5	1.5	0.5	8.246530	16.104570
	0.0	10000	1.0	1.5	0.5	0.061075	0.078267
	0.0	10000	2.0	1.5	0.5	0.063788	0.061201
	0.0	10000	1.5	1.0	0.5	0.062881	0.054239
	0.0	10000	1.5	2.0	0.5	0.061432	0.076134
	0.0	12000	1.5	1.5	0.5	0.059315	0.056257
	0.0	14000	1.5	1.5	0.5	0.060947	0.047887
	0.0	1000	1.5	1.5	0.3	0.139523	0.047492

Appendix

Case 1:

$$\begin{aligned}
 S &= \sqrt{1 - \frac{4RaRvDa^2}{Rc}}, & A &= \frac{1+S}{2DaRv}, \\
 N &= \sqrt{\frac{\sqrt{Ra}}{2}}, & B &= \frac{1-S}{2DaRv}, \\
 h_1 &= \sqrt{A}, & h_2 &= \sqrt{B}, \\
 h_3 &= h_1 d, & h_4 &= h_2 d, \\
 h_6 &= Nd, & h_7 &= 2N^2, \\
 r_1 &= \cosh(h_1), & r_2 &= \sinh(h_1), \\
 r_3 &= \cosh(h_2), & r_4 &= \sinh(h_2), \\
 r_5 &= e^{h_6} \cos(h_6), & r_6 &= e^{h_6} \sin(h_6), \\
 r_7 &= e^{-h_6} \cos(h_6), & r_8 &= e^{-h_6} \sin(h_6), \\
 r_{12} &= \sinh(h_4), \\
 r_{13} &= Ne^{h_6} \{ \cos(h_6) - \sin(h_6) \}, \\
 r_{14} &= Ne^{h_6} \{ \cos(h_6) + \sin(h_6) \}, \\
 r_{15} &= -Ne^{-h_6} \{ \cos(h_6) + \sin(h_6) \}, \\
 r_{16} &= Ne^{-h_6} \{ \cos(h_6) - \sin(h_6) \}, \\
 r_{17} &= Rvh_1 \sinh(h_3), \\
 r_{18} &= Rvh_1 \cosh(h_3), \\
 r_{19} &= Rvh_2 \sinh(h_4), \\
 r_{20} &= Rvh_2 \cosh(h_4), \\
 r_{21} &= -\frac{1}{h_7}, & r_{22} &= h_1^2 \cosh(h_1), \\
 r_{23} &= h_1^2 \sinh(h_1), & r_{24} &= h_2^2 \cosh(h_2), \\
 r_{27} &= \left(\frac{1}{Da} - Rvh_1^2 \right) \cosh(h_3), \\
 r_{28} &= \left(\frac{1}{Da} - Rvh_1^2 \right) \sinh(h_3), \\
 r_{29} &= \left(\frac{1}{Da} - Rvh_2^2 \right) \cosh(h_4), \\
 r_{30} &= \left(\frac{1}{Da} - Rvh_2^2 \right) \sinh(h_4), & r_{31} &= h_7 e^{h_6} \cos(h_6), \\
 r_{32} &= h_7 e^{h_6} \sin(h_6), & r_{33} &= h_7 e^{-h_6} \sin(h_6), \\
 r_{33} &= h_7 e^{-h_6} \sin(h_6), & r_{34} &= e^{-h_6} \cos(h_6), \\
 r_{35} &= Nh_8 e^{h_6} (\cos(h_6) - \sin(h_6)), \\
 r_{36} &= Nh_8 e^{h_6} \{ \cos(h_6) + \sin(h_6) \}, \\
 r_{37} &= Nh_8 e^{-h_6} \{ \cos(h_6) - \sin(h_6) \}, \\
 r_{38} &= Nh_8 e^{-h_6} (\cos(h_6) + \sin(h_6)), \\
 r_{39} &= \left(-Rvh_1^3 + \frac{h_1}{Da} \right) Rc \sinh(h_3), \\
 r_{40} &= \left(-Rvh_1^3 + \frac{h_1}{Da} \right) Rc \cosh(h_3), \\
 r_{41} &= \left(-Rvh_2^3 + \frac{h_2}{Da} \right) Rc \sinh(h_4), \\
 r_{42} &= \left(-Rvh_2^3 + \frac{h_2}{Da} \right) Rc \cosh(h_4), \\
 r_{43} &= -\frac{r_2}{r_1}, & r_{44} &= -\frac{r_3}{r_1}, & r_{45} &= -\frac{r_4}{r_1}, \\
 r_{46} &= r_7 - r_5, & r_{47} &= r_8 + r_6, \\
 r_{48} &= r_{10} + r_{43}r_9, & r_{49} &= r_{11} + r_{44}r_9, \\
 r_{50} &= r_{12} + r_{45}r_9, & r_{51} &= r_{21}r_6,
 \end{aligned}$$

$$\begin{aligned}
 r_{52} &= r_{15} - r_{13}, & r_{53} &= r_{14} + r_{16}, \\
 r_{54} &= r_{43}r_{17} + r_{18}, & r_{55} &= r_{44}r_{17} + r_{19}, \\
 r_{56} &= r_{45}r_{17} + r_{20}, & r_{57} &= r_{21}r_{14}, \\
 r_{58} &= r_{43}r_{22} + r_{23}, & r_{59} &= r_{44}r_{22} + r_{24}, \\
 r_{60} &= r_{45}r_{22} + r_{25}, & r_{61} &= r_{43}r_{27} + r_{28}, \\
 r_{62} &= r_{44}r_{27} + r_{29}, & r_{63} &= r_{45}r_{27} + r_{30}, \\
 r_{64} &= r_{32} + r_{33}, & r_{65} &= r_{31} - r_{34}, \\
 r_{66} &= r_{21}r_{31}, & r_{67} &= r_{35} + r_{38}, \\
 r_{68} &= r_{36} + r_{37}, & r_{70} &= r_{44}r_{39} + r_{41}, \\
 r_{69} &= r_{43}r_{39} + r_{40}, & Ar_1 &= r_{21}r_{35}, \\
 r_{71} &= r_{45}r_{39} + r_{42}, & r_{72} &= \frac{r_{26}}{r_{58}}, & r_{73} &= \frac{r_{59}}{r_{58}}, & r_{74} &= \frac{r_{60}}{r_{58}}, \\
 r_{75} &= r_{73}r_{48} - r_{49}, & r_{76} &= r_{74}r_{48} - r_{50}, \\
 r_{77} &= r_{51} - r_{72}r_{48}, & r_{78} &= r_{54}r_{73} - r_{55}, \\
 r_{79} &= r_{74}r_{54} - r_{56}, & r_{80} &= r_{57} - r_{72}r_{54}, \\
 r_{81} &= r_{62} - r_{73}r_{61}, & r_{82} &= r_{63} - r_{74}r_{61}, \\
 r_{83} &= r_{66} + r_{72}r_{61}, & r_{84} &= r_{73}r_{69} - r_{70}, \\
 r_{87} &= \frac{r_{47}}{r_{46}}, & r_{88} &= \frac{r_{75}}{r_{46}}, \\
 r_{89} &= \frac{r_{76}}{r_{46}}, & r_{90} &= \frac{r_{77}}{r_{46}}, \\
 r_{91} &= r_{53} - r_{87}r_{52}, & r_{92} &= r_{78} - r_{88}r_{52}, \\
 r_{93} &= r_{79} - r_{89}r_{52}, & r_{94} &= r_{80} - r_{90}r_{52}, \\
 r_{95} &= r_{81} - r_{88}r_{64}, & r_{96} &= r_{82} - r_{89}r_{64}, \\
 r_{97} &= r_{65} - r_{87}r_{64}, & r_{98} &= r_{83} - r_{90}r_{64}, \\
 r_{99} &= r_{67} - r_{87}r_{68}, & r_{100} &= r_{84} - r_{88}r_{68}, \\
 r_{101} &= r_{85} - r_{89}r_{68}, & r_{102} &= r_{86} - r_{90}r_{68}, \\
 r_{103} &= \frac{r_{92}}{r_{91}}, & r_{104} &= \frac{r_{93}}{r_{91}}, \\
 r_{105} &= \frac{r_{94}}{r_{91}}, & r_{106} &= r_{95} - r_{103}r_{97}, \\
 r_{107} &= r_{96} - r_{104}r_{97}, & r_{108} &= r_{98} - r_{105}r_{97}, \\
 r_{109} &= r_{100} - r_{103}r_{99}, & r_{110} &= r_{101} - r_{104}r_{99}, \\
 r_{111} &= r_{102} - r_{105}r_{99}, & r_{112} &= \frac{r_{107}}{r_{106}}, \\
 r_{113} &= \frac{r_{108}}{r_{106}}, \\
 r_{114} &= r_{110} - r_{112}r_{109}, \\
 r_{115} &= r_{111} - r_{113}r_{109}, \\
 r_{116} &= -\frac{r_{115}}{r_{114}}, & C_8 &= r_{116}, \\
 C_7 &= -(r_{112}C_8 + r_{113}), & C_6 &= r_{72} - r_{73}C_7 - r_{74}C_8, \\
 C_5 &= r_{43}C_6 + r_{44}C_7 + r_{45}C_8, \\
 C_4 &= -(r_{105} + r_{103}C_7 + r_{104}C_8), \\
 C_3 &= -(r_{90} + r_{87}C_4 + r_{88}C_7 + r_{89}C_8), \\
 C_2 &= r_{21} + C_4, & C_1 &= -C_3.
 \end{aligned}$$

Case 2:

$$\begin{aligned}
 N &= \sqrt{\frac{\sqrt{Ra}}{2}}, & S &= \sqrt{1 - \frac{4RaRvDa^2}{Rc}}, & m &= \frac{1}{2DaRv}, \\
 r_1 &= 1/2N^2, & r_2 &= \cosh m, & r_3 &= \sinh m, \\
 r_4 &= m^2 \cosh m, & r_5 &= m^2 \cosh m + 2m \sinh m,
 \end{aligned}$$

$$\begin{aligned}
 r_6 &= m^2 \sinh m, & r_7 &= 2m \cosh m + m^2 \sinh m, \\
 r_8 &= -\left(\frac{1}{Rv} + \frac{RaQ}{Rv}\right), & r_9 &= e^{Nd} \cos Nd, \\
 r_{10} &= e^{Nd} \sin Nd, & r_{11} &= e^{-Nd} \cos Nd, \\
 r_{12} &= e^{-Nd} \sin Nd, & r_{13} &= \cosh md, \\
 r_{14} &= d \cosh md, & r_{15} &= \sinh md, \\
 r_{16} &= d \sinh md, \\
 r_{17} &= Ne^{Nd} (\cos Nd - \sin Nd), \\
 r_{18} &= Ne^{Nd} (\cos Nd + \sin Nd), \\
 r_{19} &= -Ne^{-Nd} (\cos Nd + \sin Nd), \\
 r_{20} &= Ne^{-Nd} (\cos Nd + \sin Nd), \\
 r_{21} &= mRv \sinh md, \\
 r_{22} &= Rv(m \sinh md + \cosh md), \\
 r_{23} &= mRv \cosh md, \\
 r_{24} &= Rv(m \cosh md + \sinh md), \\
 r_{25} &= 2N^2 e^{Nd} \sin Nd, & r_{26} &= -2N^2 e^{Nd} \cos Nd, \\
 r_{27} &= -2N^2 e^{-Nd} \sin Nd, & r_{28} &= 2N^2 e^{-Nd} \cos Nd, \\
 r_{29} &= -Rvm^2 \cosh md + \frac{1}{Da} \cosh md, \\
 r_{30} &= -Rvm^2 d \cosh md + \frac{1}{Da} d \cosh md \\
 &\quad - 2mRv \sinh md, \\
 r_{31} &= -Rvm^2 \sinh md + \frac{1}{Da} \sinh md, \\
 r_{32} &= -Rvm^2 d \sinh md + \frac{1}{Da} d \sinh md \\
 &\quad - 2mRv \sinh md, \\
 r_{33} &= 2N^3 e^{Nd} (\sin Nd - \cos Nd), \\
 r_{34} &= 2N^3 e^{Nd} (\sin Nd + \cos Nd), \\
 r_{35} &= 2N^3 e^{-Nd} (\sin Nd - \cos Nd), \\
 r_{36} &= -2N^3 e^{-Nd} (\sin Nd - \cos Nd), \\
 r_{37} &= Rc \left(-Rvm^3 + \frac{m}{Da}\right) \sinh md, \\
 r_{38} &= Rc \left[-Rv(m^3 d \sinh md + 3m^2 \cosh md) \right. \\
 &\quad \left. + \frac{m}{Da} (m \sinh md + \cosh md)\right], \\
 r_{39} &= Rc \left(-Rvm^3 + \frac{m}{Da}\right) \cosh md, \\
 r_{40} &= Rc \left[-Rv(m^3 d \cosh md + 3m^2 \sinh md) \right. \\
 &\quad \left. + \frac{m}{Da} (\sinh md + m \cosh md)\right], \\
 r_{41} &= \frac{r_3}{r_2}, & r_{42} &= r_5 - r_4, & r_{43} &= r_6 - r_4 r_{41}, \\
 r_{44} &= r_7 - r_4 r_{41}, & r_{45} &= \frac{r_8}{r_{42}}, & r_{46} &= \frac{r_{43}}{r_{42}}, \\
 r_{47} &= \frac{r_{44}}{r_{42}}, & r_{48} &= r_{11} - r_9, & r_{49} &= r_{12} - r_{10}, \\
 r_{50} &= r_1 r_{10} + r_{45} r_{13} - r_{45} r_{14}, \\
 r_{51} &= r_{41} r_{13} - r_{46} r_{13} + r_{46} r_{14} - r_{15}, \\
 r_{52} &= r_{41} r_{13} - r_{47} r_{13} + r_{47} r_{14} - r_{16}, \\
 r_{53} &= \frac{r_{49}}{r_{48}}, & r_{54} &= \frac{r_{50}}{r_{48}}, & r_{55} &= \frac{r_{51}}{r_{48}}, \\
 r_{56} &= \frac{r_{52}}{r_{48}}, & r_{57} &= r_{20} + r_{18} - r_{53} r_{19} + r_{53} r_{17}, \\
 r_{58} &= r_{55} r_{17} - r_{23} - r_{55} r_{19} + r_{46} r_{22} - r_{46} r_{21} + r_{41} r_{21},
 \end{aligned}$$

$$\begin{aligned}
 r_{59} &= r_{56} r_{17} - r_{24} - r_{56} r_{19} + r_{22} r_{47} - r_{47} r_{21} + r_{41} r_{21}, \\
 r_{60} &= r_{54} r_{17} - r_{54} r_{19} - r_{22} r_{45} + r_{45} r_{21} + r_{18} r_{1}, \\
 r_{61} &= \frac{r_{58}}{r_{57}}, & r_{62} &= \frac{r_{59}}{r_{57}}, \\
 r_{64} &= r_{41} r_{29} - r_{31} - r_{55} r_{27} + r_{55} r_{25} - r_{29} r_{46} \\
 &\quad + r_{30} r_{46} - r_{61} r_{28} - r_{61} r_{26} + r_{61} r_{53} r_{27} \\
 &\quad - r_{61} r_{53} r_{25}, \\
 r_{65} &= r_{56} r_{25} - r_{56} r_{27} + r_{41} r_{29} - r_{32} - r_{47} r_{29} \\
 &\quad + r_{47} r_{30} - r_{62} r_{28} - r_{62} r_{26} + r_{62} r_{53} r_{27} \\
 &\quad - r_{62} r_{53} r_{25}, \\
 r_{66} &= -r_{54} r_{27} + r_{1} r_{26} + r_{54} r_{25} + r_{45} r_{29} \\
 &\quad - r_{45} r_{30} - r_{63} r_{28} - r_{63} r_{26} + r_{63} r_{53} r_{27} \\
 &\quad - r_{63} r_{53} r_{25}, \\
 r_{67} &= \frac{r_{65}}{r_{64}}, & r_{68} &= \frac{r_{66}}{r_{64}}, \\
 r_{69} &= r_{41} r_{37} - r_{56} r_{35} - r_{40} + r_{56} r_{33} - r_{47} r_{37} \\
 &\quad + r_{47} r_{38} - r_{62} r_{34} - r_{62} r_{36} + r_{62} r_{53} r_{35} \\
 &\quad - r_{62} r_{53} r_{33} - r_{67} r_{37} r_{41} + r_{67} r_{39} + r_{67} r_{55} r_{35} \\
 &\quad - r_{67} r_{33} r_{55} + r_{67} r_{46} r_{37} - r_{67} r_{38} r_{46} + r_{67} r_{61} r_{37} \\
 &\quad + r_{67} r_{61} r_{36} - r_{61} r_{53} r_{35} r_{67} + r_{67} r_{61} r_{53} r_{33}, \\
 r_{70} &= r_{68} r_{39} - r_{41} r_{68} r_{37} + r_{68} r_{55} r_{35} - r_{68} r_{33} r_{55} \\
 &\quad + r_{68} r_{46} r_{37} - r_{68} r_{38} r_{46} + r_{68} r_{61} r_{34} + r_{68} r_{61} r_{36} \\
 &\quad - r_{68} r_{61} r_{53} r_{35} + r_{68} r_{61} r_{53} r_{33} - r_{54} r_{35} + r_{33} r_{54} \\
 &\quad + r_{1} r_{34} + r_{45} r_{37} - r_{38} r_{45} r_{63} r_{34} - r_{63} r_{36} \\
 &\quad + r_{63} r_{53} r_{35} - r_{53} r_{63} r_{33}, \\
 r_{71} &= \frac{r_{70}}{r_{69}}, & C_8 &= -r_{71}, \\
 C_7 &= -(r_{68} + r_{67} C_8), & C_6 &= r_{45} - r_{46} C_7 - r_{47} C_8, \\
 C_5 &= -(C_6 + r_{41} (C_7 + C_8)), \\
 C_4 &= -(r_{61} C_7 + r_{62} C_8 + r_{63}), \\
 C_3 &= -(r_{53} C_4 + r_{55} C_7 + r_{56} C_8 + r_{54}), \\
 C_2 &= C_4 + r_1, & C_1 &= -C_3.
 \end{aligned}$$

Case 3:

$$\begin{aligned}
 R &= \sqrt{\frac{4RaRvDa^2}{Rc} - 1}, & d_1 &= \sqrt{\frac{\sqrt{1+R^2}+1}{2}}, \\
 d_2 &= \sqrt{\frac{\sqrt{1+R^2}-1}{2}}, & \alpha &= \frac{d_1}{\sqrt{2DaRv}}, \\
 \beta &= \frac{d_2}{\sqrt{2DaRv}}, & t &= \sqrt{\frac{Ra}{2}}, \\
 r_1 &= \frac{1}{2N^2}, & r_2 &= e^\alpha \cos \beta, \\
 r_3 &= e^\alpha \sin \beta, & r_4 &= e^{-\alpha} \cos \beta, \\
 r_5 &= e^{-\alpha} \sin \beta, \\
 r_6 &= \frac{e^\alpha}{DaRa} \cos \beta - \frac{Rv}{Ra} e^\alpha [(\alpha^2 - \beta^2) \cos \beta - 2\alpha\beta \sin \beta], \\
 r_7 &= \frac{e^\alpha}{DaRa} \sin \beta - \frac{Rv}{Ra} e^\alpha [(\alpha^2 - \beta^2) \sin \beta + 2\alpha\beta \cos \beta], \\
 r_8 &= \frac{e^{-\alpha}}{DaRa} \cos \beta - \frac{Rv}{Ra} e^{-\alpha} [(\alpha^2 - \beta^2) \cos \beta + 2\alpha\beta \sin \beta],
 \end{aligned}$$

$$\begin{aligned}
 r_9 &= \frac{e^{-\alpha}}{DaRa} \sin \beta - \frac{Rv}{Ra} e^{-\alpha} [(\alpha^2 - \beta^2) \sin \beta - 2\alpha\beta \cos \beta], & r_{46} &= r_7 - r_6 r_{43}, & r_{47} &= r_8 - r_6 r_{44}, \\
 r_{10} &= \frac{T_1 - T_0}{AHQ} - \frac{1}{Ra}, & r_{11} &= e^{Nd} \cos Nd, & r_{48} &= r_9 - r_6 r_{45}, & r_{49} &= \frac{r_{10}}{r_{46}}, \\
 r_{12} &= e^{Nd} \sin Nd, & r_{13} &= e^{-Nd} \cos Nd, & r_{50} &= \frac{r_{47}}{r_{46}}, & r_{51} &= \frac{r_{48}}{r_{46}}, \\
 r_{14} &= e^{-Nd} \sin Nd, & r_{15} &= e^{\alpha d} \cos \beta d, & r_{52} &= r_{13} - r_{11}, & r_{53} &= r_{14} + r_{12}, \\
 r_{16} &= e^{\alpha d} \sin \beta d, & r_{17} &= e^{-\alpha d} \cos \beta d, & r_{54} &= r_1 r_{12} + r_{49} r_{43} r_{15} - r_{49} r_{16}, \\
 r_{18} &= e^{-\alpha d} \sin \beta d, & r_{19} &= \frac{2N^2}{Ra} e^{Nd} \sin Nd, & r_{55} &= r_{44} r_{15} - r_{17} - r_{50} r_{43} r_{15} + r_{50} r_{16}, \\
 r_{20} &= -\frac{2N^2}{Ra} e^{Nd} \cos Nd, & & & r_{56} &= r_{45} r_{15} - r_{18} - r_{51} r_{43} r_{15} + r_{51} r_{16}, \\
 r_{21} &= -\frac{2N^2}{Ra} e^{-Nd} \sin Nd, & & & r_{57} &= \frac{r_{53}}{r_{52}}, & r_{58} &= \frac{r_{54}}{r_{52}}, & r_{59} &= \frac{r_{55}}{r_{52}}, \\
 r_{22} &= \frac{2N^2}{Ra} e^{-Nd} \cos Nd, & & & r_{60} &= \frac{r_{56}}{r_{52}}, & r_{61} &= r_{22} + r_{20} - r_{21} r_{57} + r_{19} r_{57}, \\
 r_{23} &= \frac{e^{\alpha d}}{DaRa} \cos \beta - \frac{Rv}{Ra} e^{\alpha d} [(\alpha^2 - \beta^2) \cos \beta d - 2\alpha\beta \sin \beta d], & r_{62} &= r_{44} r_{23} - r_{25} - r_{21} r_{59} + r_{19} r_{59} - r_{50} r_{43} r_{23} + r_{24} r_{50}, \\
 r_{24} &= \frac{e^{\alpha}}{DaRa} \sin \beta d - \frac{Rv}{Ra} e^{\alpha d} [(\alpha^2 - \beta^2) \sin \beta d + 2\alpha\beta \cos \beta d], & r_{63} &= -r_{60} r_{21} + r_{60} r_{19} + r_{45} r_{23} r_{26} - r_{51} r_{43} r_{23} + r_{24} r_{51}, \\
 r_{25} &= \frac{e^{-\alpha d}}{DaRa} \cos \beta d - \frac{Rv}{Ra} e^{-\alpha d} [(\alpha^2 - \beta^2) \cos \beta d + 2\alpha\beta \sin \beta d], & r_{64} &= -r_{58} r_{21} + r_{58} r_{19} + r_1 r_{20} + r_{49} r_{43} r_{23} - r_{49} r_{24}, \\
 r_{26} &= \frac{e^{-\alpha d}}{DaRa} \sin \beta d - \frac{Rv}{Ra} e^{-\alpha d} [(\alpha^2 - \beta^2) \sin \beta d - 2\alpha\beta \cos \beta d], & r_{66} &= \frac{r_{63}}{r_{61}}, & r_{67} &= \frac{r_{64}}{r_{61}}, \\
 r_{27} &= Ne^{Nd} (\cos Nd - \sin Nd), & r_{68} &= r_{44} r_{31} - r_{33} - r_{29} r_{59} + r_{59} r_{27} - r_{65} r_{28} \\
 & & & & & & & & & -r_{30} r_{65} + r_{65} r_{57} r_{29} - r_{57} r_{27} r_{65} - r_{50} r_{43} r_{31} \\
 & & & & & & & & & + r_{50} r_{32}, \\
 r_{28} &= Ne^{Nd} (\cos Nd + \sin Nd), & r_{69} &= r_{45} r_{31} - r_{34} - r_{66} r_{29} + r_{60} r_{27} - r_{66} r_{28} \\
 & & & & & & & & & -r_{66} r_{30} + r_{57} r_{29} r_{66} - r_{57} r_{27} r_{66} - r_{43} r_{31} r_{51} \\
 & & & & & & & & & + r_{32} r_{51}, \\
 r_{29} &= -Ne^{-Nd} (\cos Nd + \sin Nd), & r_{70} &= r_1 r_{28} - r_{58} r_{29} + r_{58} r_{27} - r_{67} r_{28} - r_{67} r_{30} \\
 & & & & & & & & & + r_{67} r_{57} r_{29} - r_{67} r_{57} r_{27} + r_{49} r_{43} r_{31} - r_{32} r_{49}, \\
 r_{30} &= Ne^{-Nd} (\cos Nd - \sin Nd), & r_{71} &= \frac{r_{69}}{r_{68}}, & r_{72} &= \frac{r_{70}}{r_{68}}, \\
 r_{31} &= Rve^{\alpha d} (\alpha \cos \beta d - \beta \sin \beta d), & r_{73} &= r_{44} r_{39} - r_{41} - r_{59} r_{37} + r_{59} r_{35} + r_{65} r_{57} r_{37} \\
 & & & & & & & & & -r_{65} r_{57} r_{35} - r_{65} r_{36} - r_{38} r_{65} - r_{50} r_{43} r_{39} + r_{50} r_{40}, \\
 r_{32} &= Rve^{\alpha d} (\beta \cos \beta d + \alpha \sin \beta d), & r_{74} &= r_{45} r_{39} - r_{42} - r_{60} r_{37} + r_{60} r_{35} + r_{66} r_{57} r_{37} \\
 & & & & & & & & & -r_{66} r_{57} r_{35} - r_{66} r_{36} - r_{38} r_{66} - r_{51} r_{43} r_{39} \\
 r_{33} &= -Rve^{-\alpha d} (\alpha \cos \beta d + \beta \sin \beta d), & & & & & & & & + r_{51} r_{40}, \\
 r_{34} &= -Rve^{-\alpha d} (\beta \cos \beta d - \alpha \sin \beta d), & r_{75} &= r_1 r_{36} - r_{58} r_{37} + r_{58} r_{35} + r_{67} r_{57} r_{37} - r_{67} r_{57} r_{35} \\
 & & & & & & & & & -r_{67} r_{56} - r_{38} r_{67} + r_{49} r_{43} r_{39} - r_{40} r_{49}, \\
 r_{35} &= \frac{2N^3}{Ra} e^{Nd} (\cos Nd + \sin Nd), & r_{76} &= r_{74} - r_{71} r_{73}, & r_{77} &= r_{75} - r_{72} r_{73}, \\
 r_{36} &= \frac{2N^3}{Ra} e^{Nd} (\sin Nd - \cos Nd), & r_{78} &= \frac{r_{77}}{r_{76}}, & C_8 &= -r_{78}, \\
 r_{37} &= \frac{2N^3}{Ra} e^{-Nd} (\sin Nd - \cos Nd), & C_7 &= -(r_{71} C_8 + r_{72}), & C_6 &= r_{49} - r_{50} C_7 - r_{51} C_8 \\
 r_{38} &= -\frac{2N^3}{Ra} e^{Nd} (\cos Nd + \sin Nd), & C_5 &= -(r_{43} C_6 + r_{44} C_7 + r_{45} C_8), \\
 r_{39} &= Rce^{\alpha d} \left\{ \frac{1}{DaRa} (\alpha \cos \beta d - \beta \sin \beta d) - \frac{Rv}{Ra} \right. \\
 & & & & & & & & & \left. [(\beta^3 - 3\alpha^2 \beta) \sin \beta d + (\alpha^3 - 3\alpha\beta^2) \cos \beta d] \right\}, \\
 r_{40} &= Rce^{\alpha d} \left\{ \frac{1}{DaRa} (\beta \cos \beta d + \alpha \sin \beta d) - \frac{Rv}{Ra} \right. \\
 & & & & & & & & & \left. [(3\alpha^2 \beta - \beta^3) \cos \beta d + (\alpha^3 - 3\alpha\beta^2) \sin \beta d] \right\}, \\
 r_{41} &= \{-Rce^{-\alpha d} \left\{ \frac{1}{DaRa} (\alpha \cos \beta d + \beta \sin \beta d) \right\} - \frac{Rv}{Ra} \right. \\
 & & & & & & & & & \left. [(\beta^3 - 3\alpha^2 \beta) \sin \beta d + (3\alpha\beta^2 - \alpha^3) + \cos \beta d] \right\}, \\
 r_{42} &= Rce^{-\alpha d} \left\{ -\frac{1}{DaRa} (\beta \cos \beta d - \alpha \sin \beta d) - \frac{Rv}{Ra} \right. \\
 & & & & & & & & & \left. \{ (3\alpha^2 \beta - \beta^3) \cos \beta d + (3\alpha\beta^2 - \alpha^3) + \sin \beta d \} \right\}, \\
 r_{43} &= \frac{r_3}{r_2}, & r_{44} &= \frac{r_4}{r_2}, & r_{45} &= \frac{r_5}{r_2},
 \end{aligned}$$